J|A|C|S ARTICLES

Published on Web 04/28/2010

Hydrogenation-Induced Surface Polarity Recognition and Proton Memory Behavior at Protic-Ionic-Liquid/Oxide Electric-Double-Layer Interfaces

Hongtao Yuan,*[,†,‡] Hidekazu Shimotani,[†,‡] Atsushi Tsukazaki,[†] Akira Ohtomo,[†] Masashi Kawasaki,[†,‡,$] and Yoshihiro Iwasa*[,†,‡]

Institute for Materials Research, Tohoku University, Sendai 980-8577, Japan, Japan Science and Technology Agency (CREST), Kawaguchi 332-0012, Japan, and WPI Advanced Institute for Materials Research, Tohoku University, Sendai 980-8577 Japan

Received October 26, 2009; E-mail: htyuan@imr.tohoku.ac.jp; iwasa@imr.tohoku.ac.jp

Abstract: The electric-double-layer (EDL) formed at liquid/solid interfaces provides a broad and interdisciplinary attraction in terms of electrochemistry, photochemistry, catalysts, energy storage, and electronics. Especially in recent years, much effort has been devoted to the fundamental understanding and practical applications of transistor configurations with EDLs because of their ability for high-density charge accumulation. However, to exploit additional new functionalities of such an emerging interface is not only of great importance but also a huge challenge. Here, we demonstrate that, by introducing protic ionic liquid (PIL) as the gate dielectric for ZnO EDL transistors (EDLTs), small and chemically active ions, such as protons and hydroxyls, can serve as an adsorption medium to extend the interfacial functionalities of EDLTs. By selectively driving the H^+ or OH^- groups onto ZnO channel surfaces with an electric field, the charged adsorbates interact with surface atoms in different adsorption mechanisms, showing remarkable variations in electron transport and providing a possibility for the recognition of surface polarity. Most significantly, the large hysteresis in the transfer characteristics of PIL−EDLTs makes the device available and promising for nonvolatile proton memory devices via surface hydrogenation and dehydrogenation processes. Such a finding provides us with new opportunities to understand liquid/solid heterogeneous interface phenomena and to extend the practical functions of EDLs through controllable interfacial interaction.

Introduction

As a category of emerging organic salts, ionic liquids (IL) show a broad interest in electrochemistry, photochemistry, catalysis, electronics, and clean energy as well as the interdisciplinary richness it raises on both fundamental and applied levels.[1−8] The electric-double-layer (EDL) at IL/solid interface, functioning as a nanoscale capacitor with a huge capacitance, has recently attracted extensive attention because of its remarkable capability for high-density charge accumulation in the field-effect transistor (FET) configuration.[1−15] Figure 1a diagrams a cross section of such an EDL interface using an ionic liquid as the gate dielectric for an EDL transistor. When a gate voltage is applied between the gate electrode and a semiconductor surface, the mobile cation and anion will move toward oppositely charged electrodes to form EDLs by screening high-density carriers at the solid side. Because of the large capacitance coupling at EDL interfaces, remarkable progress has been achieved not only in practical transistor applications,[1,12,14] but also in the electrostatic modulation of electronic states of channel materials as exemplified by insulator-to-metal phase transitions[10,11,15] and electric-field-induced superconductivity in oxide and nitride semiconductors.[2,3]

Normally, at the EDL interface, the IL ions interact with the solid surface simply by electrostatic or van der Waals interaction

† IMR. Tohoku University.
‡ CREST, JST.
$ WPI-AIMR, Tohoku University.

(1) Cho, J. H.; Lee, J.; Xia, Y.; Kim, B. S.; He, Y.; Renn, M. J.; Lodge, T. P.; Frisbie, C. D. *Nat. Mater.* **2008**, *7*, 900–906.
(2) Ueno, K.; Nakamura, S.; Shimotani, H.; Ohtomo, A.; Kimura, N.; Nojima, T.; Aoki, H.; Iwasa, Y.; Kawasaki, M. *Nat. Mater.* **2008**, *7*, 855–858.
(3) Ye, J. T.; Inoue, S.; Kobayashi, K.; Kasahara, Y.; Yuan, H. T.; Shimotani, H.; Iwasa, Y. *Nat. Mater.* **2010**, *9*, 125–128.
(4) Shimotani, H.; Diguet, G.; Iwasa, Y. *Appl. Phys. Lett.* **2005**, *86*, 022104−1-3.
(5) Panzer, M. J.; Frisbie, C. D. *J. Am. Chem. Soc.* **2005**, *127*, 6960–6961.
(6) Takeya, J.; Yamada, K.; Hara, K. *Appl. Phys. Lett.* **2006**, *88*, 112102–1-3.
(7) Panzer, M. J.; Frisbie, C. D. *Appl. Phys. Lett.* **2006**, *88*, 203504–1-3.
(8) Dhoot, A. S.; Yuen, J. D.; Heeney, M.; McCulloch, I.; Moses, D.; Heeger, A. J. *Proc. Natl. Acad. Sci. U.S.A.* **2006**, *103*, 11834–11837.
(9) Herlogsson, L.; Crispin, X.; Rohinson, N. D.; Sandberg, M.; Hagel, O. J.; Gustafsson, G.; Berggren, M. *Adv. Mater.* **2007**, *19*, 97–101.
(10) Shimotani, H.; Asanuma, H.; Tsukazaki, A.; Ohtomo, A.; Kawasaki, M.; Iwasa, Y. *Appl. Phys. Lett.* **2007**, *91*, 082106−1-3.
(11) Misra, R.; McCarthy, M.; Hebard, A. F. *Appl. Phys. Lett.* **2007**, *90*, 052905−1-3.
(12) Lee, J.; Panzer, M. J.; He, Y.; Lodge, T. P.; Frisbie, C. D. *J. Am. Chem. Soc.* **2007**, *129*, 4532–4533.
(13) Cho, J. H.; Lee, J.; He, Y.; Kim, B. S.; Lodge, T. P.; Frisbie, C. D. *Adv. Mater.* **2008**, *20*, 686–690.
(14) Ono, S.; Seki, S.; Hirahara, R.; Tominari, Y.; Takeya, J. *Appl. Phys. Lett.* **2008**, *92*, 103313–1-3.
(15) Yuan, H. T.; Shimotani, H.; Tsukazaki, A.; Ohtomo, A.; Kawasaki, M.; Iwasa, Y. *Adv. Funct. Mater.* **2009**, *19*, 1046–1053.

 10.1021/ja909110s

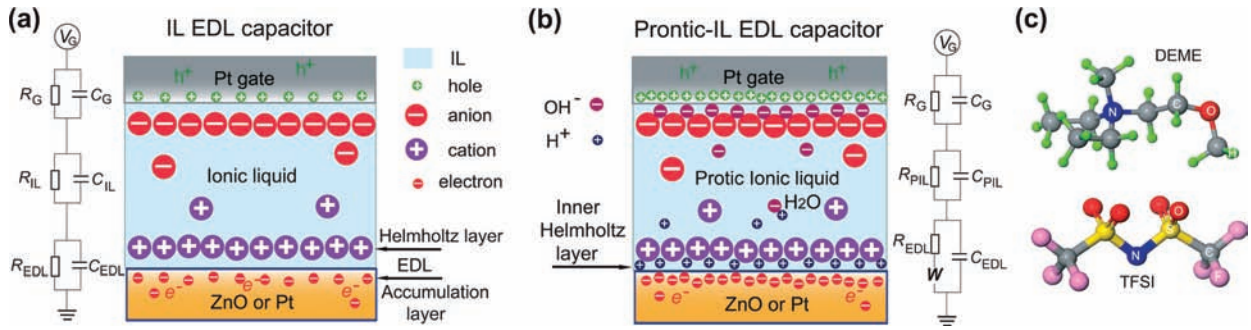

Figure 1. Schematic structures of IL and PIL gated EDLTs. (a) Cross section diagram of an IL/solid EDL capacitor. The equivalent circuit can be regarded as three resistor−capacitor (RC) circuits in series: two RCs for the EDL interfaces at the electrodes and one for the bulk IL phase. (b) Cross section diagram of a PIL/solid EDL capacitor. Under a positive gate bias, the H^+ cations will accumulate at the anode to form an inner Helmholtz layer while the OH^- anions will accumulate at the cathode, corresponding to surface hydrogenation and hydroxylation, respectively. (c) Molecular structure of the IL (DEME-TFSI) used in this work.

without any chemical bonding[16−18] due to their inert chemical reactivity within the electrochemical potential windows.[11,19,20] This is the reason the charge accumulation at the EDL interface in a transistor usually occurs in an electrostatic manner, providing fast and reversible charge/discharge processes with a long device life[1] rather than some slow irreversible electrochemical process. In addition, at the EDL interface, the molecular size of the accumulated ions has a direct influence on the EDL capacitance coupling, where a smaller ion size results in a larger EDL capacitance with a relatively higher interfacial charge density. So far, the function of EDLTs is usually limited to charge accumulation and modulation for FET operation because of the above-mentioned inert chemical reactivity and large molecular size of ILs, both of which make the IL ions lose the ability to probe surface information of the transport channels. However, if some reactive ions with small ion sizes such as protons (H^+) and hydroxyls (OH^-) could be driven to the IL/solid interface, a resulting strong interaction between the ions and the solid surface is expected to be able to probe the surface properties and provide the EDLTs with some new functions.

In the present research, by introducing protic ionic liquid (PIL) as the gate dielectric, we report new extended functionalities of EDL transistors including surface atom recognition and proton memory performance. The PIL we used here is a kind of IL doped with a weak Brønsted acid to form a proton and a related base as the additional mobile ions.[21,22] Being a simple weak Brønsted acid, H_2O was selected as the dopant because the water molecules in ILs are known to electrostatically dissociate into protons and hydroxyls,[23,24] both of which have smaller ion sizes and relatively high chemical reactivities. In such a case, the PIL−EDLT (cross section displayed in Figure 1b) might serve not only as a metal-insulator-semiconductor FET, but also as a water electrolysis cell for the cogeneration of protons and hydroxyls.[23,24] ZnO was chosen as a channel material in this study since it is a well-known archetypal oxide semiconductor with relatively high mobility and available atomically flat surfaces. In particular, ZnO has a wurtzite structure, which in nature has polar surfaces with different surface atom terminations (the O-terminated $(000\bar{1})$ face, denoted here "ZnO-O", and the Zn-terminated (0001) face, denoted "ZnO-Zn"). The polarization-induced net surface charges and the resulting large surface energies[25] make the surface atoms more sensitive and active to the charged ions from PILs. When the dissociated H^+ and OH^- ions are selectively driven to ZnO polar surfaces and pushed inside the EDL through positive (or negative) gate bias, the H^+ (or OH^-) ions interact with the surface atoms and act as inner Helmholtz layers. Importantly, these inner Helmholtz layers can provide some unique and interesting functions that are not expected in standard IL−EDLTs: (a) the reduced capacitor gap and the increased ion density at the interface enlarge EDL capacitance; (b) variations in surface adsorption mechanisms give the H^+ and OH^- groups a fingerprint identification function to distinguish surface atom terminations; and (c) the reversible surface adsorption−desorption of the protons endows the PIL−EDLTs with a proton memory behavior. Promisingly, these novel phenomena provide new opportunities to understand liquid/solid interfacial charge transport and to extend the functionality of EDLTs through controllable interfacial interaction.

Experimental Section

The ionic liquid used in this study was *N*,*N*-diethyl-*N*-(2-methoxyethyl)-*N*-methylammonium bis-trifluoromethylsulfonyl)-imide (DEME-TFSI) from Kanto Chemical Co. The molecular structure is shown in Figure 1c. The protic IL was formed from neat IL by doping with a small amount of weak Brønsted acid, H_2O. To dissolve water in IL with a constant quantity, we put neat IL into flowing N_2 gas with a constant relative humidity rather than directly dropping water into IL. In this case, the H^+ and OH^- groups were not only effectively produced in bulk PIL, but also limited to within a safe amount of water molecules to prevent chemical processes with bulk solid. By simply controlling the humidity of the N_2 carrier gas, we could accurately and reversibly attain a H_2O concentration c_{H2O} in IL in a range from 5 to 5000 ppm, which values were quantified by the coulometric Karl Fischer titration method using a Hiranuma AQ-200 apparatus. In this research, the c_{H2O} was fixed at a level around 500 ppm.

(16) Lynden-Bell, R. M.; Del Popolo, M. G.; Youngs, T. G. A.; Kohanoff, J.; Hanke, C. G.; Harper, J. B.; Pinilla, C. *Acc. Chem. Res.* **2007**, *40*, 1138–1145.
(17) Kornyshev, A. A. *J. Phys. Chem. B* **2007**, *111*, 5545–5557.
(18) Pinilla, C.; Del Pópolo, M. G.; Kohanoff, J.; Lynden-Bell, R. M. *J. Phys. Chem. B* **2007**, *111*, 4877–4884.
(19) Welton, T. *Chem. Rev.* **1999**, *99*, 2071–2084.
(20) Susan, M. A. B. H.; Kaneko, T.; Noda, A.; Watanabe, M. *J. Am. Chem. Soc.* **2005**, *127*, 4976–4983.
(21) Greaves, T. L.; Drummond, C. J. *Chem. Rev.* **2008**, *108*, 206–237.
(22) Fumino, K.; Wulf, A.; Ludwig, R. *Angew. Chem., Int. Ed.* **2009**, *48*, 3184–3186.
(23) Fujishima, A.; Honda, K. *Nature* **1972**, *238*, 37–38.
(24) Eikerling, M.; Kornyshev, A. A.; Kucernak, A. R. *Phys. Today* **2006**, *59*, 38–44.
(25) Noguera, C. *J. Phys.: Condens. Matter* **2000**, *12*, R367–R410.

This amount of water dopant should be sufficient for affecting the transport properties of ZnO channel surfaces. Although there remain several uncertainties, for example, the acid−base equilibrium or the dissociation degree of water in electrochemical cells, arising from the nonuniform distribution of H^+ and OH^- between bulk solution and near the two electrodes, the quantitative estimation for the number of involved protons at EDL interface still can be done. Simply assuming that the dissociation degree of water in PILs is 50%,[26] the total amount of protons in the 0.4 mL of PIL with a water doping level of 500 ppm is estimated as 2×10^{17}. If only 0.1% of these protons are condensed on top of the channel surface with a typical area of 500 μm $\times$ 300 μm, the proton density on the channel surface will be 1.4×10^{17} cm^{-2}, which is more than 2 orders of magnitude larger than that of the accumulated carrier density in IL/ZnO EDLTs (the maximum value reported so far is 8×10^{14} cm^{-2}).[15] Also, there is a gas/solution solubility balance between moisture gas and PIL, which can keep the water doping level in bulk PIL (500 ppm in this research) and continuously provide enough dissociated water groups, H^+ and OH^-, to the interface.

The EDLT fabrication processes were the same as in our previous reports.[10,15] EDLTs on both ZnO-Zn and ZnO-O surfaces were systematically examined. EDL charging processes were investigated in detail by electrochemical impedance spectroscopy using a ZAHNER Elektrik IM6eX impedance spectrum analyzer. On both Pt/IL/Pt and Pt/IL/ZnO sandwiched structures, the capacitance measurement was performed with an applied AC voltage of 5 mV (frequency range from 10 mHz to 1 MHz). The EDL capacitance C_{EDL} was derived from the equation: $C_{EDL} = 1/(2\pi fZ'')$, where f is the frequency and Z'' is the imaginary part of the impedance. Note that the counter gate electrode is designed to have a much larger surface area than that of the working electrode. In this case, the additional reference electrode becomes unnecessary since most of the gate potential will drop at the working electrode interface, whether it is Pt or ZnO. The capacitance of the EDL formed at the gate electrode will be significantly large in the equivalent circuit, indicating that the measured EDL capacitance dominantly comes from the contribution of the EDL capacitor C_{EDL} at the working electrode. The transport behavior of the PIL−EDL transistors was measured in a vacuum chamber with flowing N_2 carrier gas, which is different from that of the IL−EDL transistors measured in a vacuum or dry N_2 atmosphere. An Agilent 5270B semiconductor parameter analyzer was used to measure the transport characteristics of the EDL transistors by a four-probe method with a V_G sweep speed of 20 mV s^{-1}.

Results and Discussion

Capacitance Enhancement by Using PIL. The most direct influence of PIL on the performance of EDLTs is that the reduced capacitor gap and increased ion density at the interface enlarge the EDL capacitance. To clarify the roles of the H^+ and OH^- groups on the interfacial charging and capacitance coupling, electrochemical impedance spectroscopy was performed on sandwiched Pt/liquid/Pt and Pt/liquid/ZnO structures. Figure 2a shows the frequency profiles of the specific EDL capacitance in the Pt/liquid/Pt configuration. The capacitance, $C_{PIL\text{-}EDL}$ (using PIL as the dielectric), increases dramatically to 2000 μF/cm^2 with the frequency decreasing to 10 mHz. Compared to the $C_{IL\text{-}EDL}$, less than 100 μF/cm^2 in IL dielectric cases, the PIL−EDL has a much larger capacitance.

In the equivalent electric circuit of IL−EDLT, as shown in the left panel of Figure 1a, the Pt/liquid/Pt structure can be regarded as a series of three resistor−capacitor (RC) circuits:

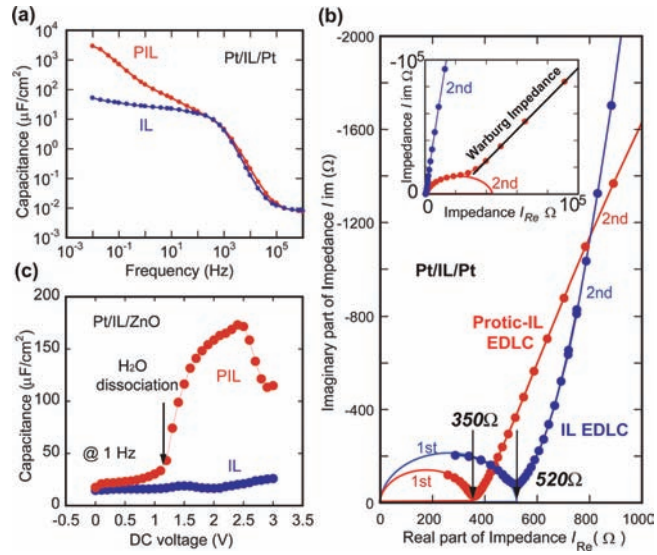

Figure 2. Comparison of the capacitance and impedance measurements between IL−EDLTs and PIL−EDLTs. (a) Frequency dependence of EDL capacitance. The capacitance at a frequency lower than 100 Hz is dramatically enhanced in the PIL case, caused by the formation of the H^+ (or OH^-) inner Helmholtz layer. (b) High frequency part of the Cole−Cole plot. The dots are the obtained data and the solid line is to guide the eyes. The first semicircle at high-frequency response corresponds to the resistance of bulk dielectric in parallel with its geometric capacitance, as shown in the RC circuits of Figure 1a,b. The inset shows the low frequency part of the Cole−Cole plot with the additional Warburg impedance in the PIL case. (c) DC voltage dependence of capacitance in IL−EDLTs and PIL−EDLTs. The capacitance of PIL−EDLTs is drastically enhanced by H_2O dissociation at 1.23 V (the standard electrode potential).

two RCs for the EDLs formed at the gate electrode and channel, and one for the bulk IL phase. This standard scenario for the EDL carrier accumulation can further help us understand why the capacitance is greatly enlarged and why only at low frequency.

(a) In the case of electrostatic charging, time constant, $\tau = RC$, is the key parameter for the charging dynamics. Note that different RC coupling has its own time domain (namely, the frequency domain), which strongly depends on the absolute values of R and C elements, and can be directly reflected from the $C - f$ plot. It can be seen from Figure 2a that the geometrical capacitance of bulk IL functioning as a small capacitance, C_{IL}, has a quick time constant at high frequency, whereas the RC coupling of EDL causes a very large time constant due to its large capacitance. So, it is always the case that the EDL related capacitance, whether is induced by the IL or the PIL, just occurs at low frequency region.

(b) Second, at the PIL/ZnO interface, Faradaic charge (Q_F) passed through interfaces in an electro-sorption process or in a surface redox process is always a function of gate potential. Then, the derivative, dQ_F/dV, causes an additional capacitance. Such a capacitance is Faradaic in origin and has a slow responding speed, being referred as a *pseudocapacitance*.[27,28] In contrast to the EDL capacitor in an electrostatic way, the pseudocapacitance accumulates charges from the Faradaic electron-transfer process at a lower frequency, where the capacitance is well described by a phenomenological relationship, $C = (1/2)\sigma^{-1}\omega^{-1/2}$ (σ is a parameter related with the

(26) Zhao, C.; Burrell, G.; Torriero, A. A. J.; Separovic, F.; Dunlop, N. F.; MacFarlane, D. R.; Bond, A. M. *J. Phys. Chem. B* **2008**, *112*, 6923–6936.
(27) Aricò, A. S.; Bruce, P.; Scrosati, B.; Tarascon, J. M.; Schalkwijk, W. V. *Nat. Mater.* **2005**, *4*, 366–377.
(28) Simon, P.; Gogotsi, Y. *Nat. Mater.* **2008**, *7*, 845–854.

Warburg impedance). From the above considerations, the large enhancement of capacitance is predominantly attributed to the pseudocapacitance rather than to electrostatic charging. The contribution of electrostatic capacitance will be discussed later in the transfer curve measurements.

The Cole−Cole plots of EDL impedance, shown in Figure 2b in the form of the well-known shape of two semicircles,[29−32] clearly displays that the ionic conductivity of ILs increases after introducing water. The resistance, R_b, of the bulk dielectrics (indicated by arrows in Figure 2b) can be directly seen from the diameter of the first semicircle at the high-frequency response. A definite decrease in R_b from 520 to 350 Ω, in other words, an increase in the ionic conductivity of the dielectric liquid, is observed when water is introduced into the neat IL. Although it has been well documented in the literature[33] that the addition of water will reduce the viscosity and lead to an increase in conductivity, in our particular case, the doping level of water in the IL (using a moist atmosphere rather than directly dropping water) is as little as around 500 ppm. In such a very light doping region, the influence of water on the viscosity and further on the conductivity of IL can be ignored. Thus, the decrease in R_b unambiguously confirms that the newly formed H^+ and OH^- actually act as additional mobile ions for improving the conductivity of the dielectric liquid, which is crucial for the fast polarization of liquid dielectrics in fast-switching devices.

In the case of neat IL, the second semicircle with a very large diameter along the *x*-axis (real part of impedance) indicates the large resistivity and excellent insulating behavior at the IL−EDL interface. On the other hand, in the case of PIL, the diameter of the second semicircle becomes much smaller, suggesting poor insulating property at the PIL−EDL interface where the gate current is considerably enhanced (discussed later). Actually, a mass transfer impedance (namely, the Warburg impedance, *W*), showing the vector with identical real and imaginary components (inset of Figure 2b), can be another piece of evidence for the diffusion of H^+ (or OH^-) near the PIL−EDL interface and the resulting enhancement of the pseudocapacitance at low frequency.[25,34,35] Since the small-size H^+ (or OH^-) in the bulk PIL−EDL is much easier to be electrically driven to the PIL−EDL interface than other ions, a mass transfer impedance, which means a diffusion of electro-active ions (H^+ or OH^-) from bulk to the interface, can be observed at the low-frequency part of the complex impedance.

Such water-dissociation enhanced capacitance can be further proved by the DC voltage dependence of capacitance in the Pt/liquid/ZnO structure, as displayed in Figure 2c. From the blue curve, one can see that the capacitance of the IL−EDLT device at 1 Hz is almost constant when V_G goes from 0 to 3 V. In remarkable contrast, the capacitance of the PIL−EDLT device exhibits a sudden increase to a large value of more than 170 $\mu F/cm^2$ (red curve). Note that the abrupt increase occurs around

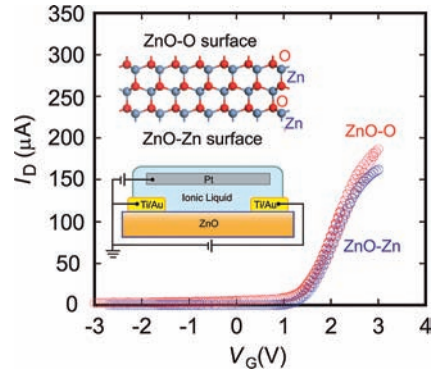

Figure 3. Transfer characteristics of IL−EDLTs on ZnO-Zn and ZnO-O surfaces measured with a drain voltage, V_D, of 100 mV. Top inset, atomic structure model of ZnO polar surfaces; bottom inset, device configuration of EDLTs. Basically, there is no obvious difference in the electron transport between the IL−EDLTs on the two polar surfaces.

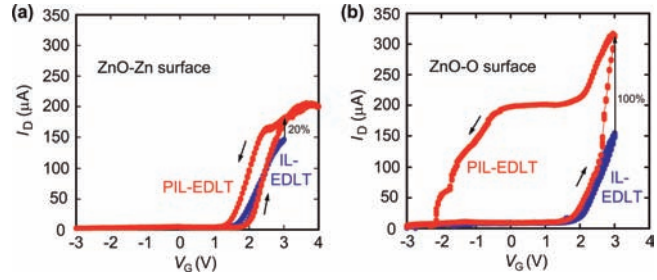

Figure 4. (a and b) Transfer characteristics of PIL−EDLTs on ZnO-Zn and ZnO-O surfaces, respectively. In the cases of PIL−EDLTs, the transport characteristics show quite different behaviors between the two surfaces.

1.2 V, which is identical to the standard electrode potential for water electrolysis (1.23 V), implying that the dissociation of water directly enhances capacitance coupling in the PIL−EDLTs.

Surface Polarity and Surface Atom Recognition by Controllable Hydrogenation and Hydroxylation on Polar ZnO. Figure 3 shows the transfer curves, drain current I_D versus gate voltage V_G, of the EDLTs with neat IL. On both ZnO-Zn and ZnO-O surfaces, the typical *n*-type transistor operation was observed with electron accumulation at positive V_G and electron depletion at negative V_G. No obvious variation in electron transport could be found on different polar surfaces and the characteristics are always similar, including the threshold voltage, the on−off ratio, the hysteresis-free behavior, and the considerably small leak current (3 orders of magnitude smaller than the channel current). Because of the polar nature of ZnO crystals (the O-terminated surface and Zn-terminated surface, as specified by crystal orientation and termination atom; surface atom structure is shown in the inset of Figure 3), the polarity dependent response of device performance has been anticipated in the EDLTs on both polar surfaces. However, as shown in Figure 3, the device performance was found to be polarity insensitive, possibly due to the inert interaction between IL molecules and ZnO surface atoms.

In contrast, after putting the IL−EDLTs into the controllable moisture condition to form the PIL−EDLTs, we observed a remarkable dependence of electron transport on the surface polarity of ZnO, which is quite different from the results above in IL−EDLTs. Panels a and b of Figure 4 show the transfer characteristics of the PIL−EDLTs fabricated on the ZnO-Zn and ZnO-O surfaces, respectively. Both surfaces showed a common increase of channel current, I_D, upon exposure of the

(29) Rehbach, M. S. *Pure Appl. Chem.* **1994**, *66*, 1831–1891.
(30) Jiang, J.; Kucernak, A. *J. Electroanal. Chem.* **2000**, *490*, 17–30.
(31) Kornyshev, A. A., Spohr, E., Vorotyntsev, M. A., Electrochemical Double Layers, In: *Encyclopedia of Electrochemistry, V1: Thermodynamics and Electrified Interfaces*; Wiley-VCH, New York, 2002.
(32) Vorotyntsev, M. A.; Badiali, J. P.; Inzelt, G. *J. Electroanal. Chem.* **1999**, *472*, 7–19.
(33) Kelkar, M. S.; Maginn, E. J. *J. Phys. Chem. B* **2007**, *111*, 4867–4876.
(34) Brown, G. E., Jr. *Science* **2001**, *294*, 67–69.
(35) Salmeron, M.; Bluhm, H.; Tatarkhanov, M.; Ketteler, G.; Shimizu, T. K.; Mugarza, A.; Deng, X.; Herranz, T.; Yamamoto, S.; Nilsson, A. *Faraday Discuss.* **2009**, *141*, 221–229.

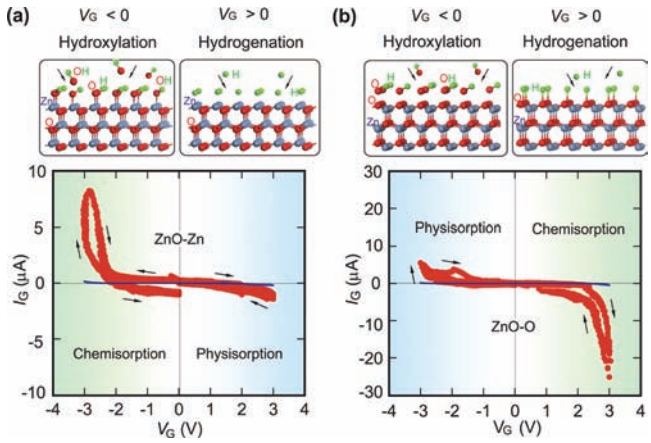

Figure 5. (a and b) I_G versus V_G of PIL−EDLTs on ZnO-Zn and ZnO-O surfaces, respectively. Top panels: atomic structure models of chemisorption and physisorption on the hydrogenated and hydroxylated surfaces.

device to moisture, whereas they also displayed contrasting behavior in transfer characteristics. The first difference is the increased amount of current response by introducing water. Compared to the 20% increase of I_D at V_G of 3 V in the case of ZnO-Zn, the I_D value at the same V_G on the ZnO-O surface always increased in magnitude by several hundred percent. For example (shown in Figure 4b), the I_D increase in the EDLT on the ZnO-O surface reached 100%. The second difference is the hysteresis of the transfer curves. On the ZnO-Zn surface, a small hysteresis with a threshold voltage (V_{th}) shift of less than 0.4 V was observed, whereas in the case of ZnO-O, we found a large hysteresis of more than 3 V in width together with highly conductive flat transfer characteristics. This large hysteresis indicates a potential functionality of EDLTs for nonvolatile memory devices by using PIL gating, which will be discussed later.

It should be noted here that the increases of conductivity in PIL−EDLTs shown in Figure 4 are significantly smaller than the capacitance increase in Figure 2a. This dramatic difference between capacitance enhancement and channel conductivity enhancement indicates that the capacitance enhancement in the low frequency region in Figure 2a is dominated by the pseudocapacitance, which originates from electrochemical adsorption. Most of the involved Faradaic charges are trapped at the interface but still slightly contribute to the channel current. The contribution to the electrostatic capacitance of the protons in the inner Helmholtz layer manifests itself, in a first-order approximation, in the 20% channel current enhancement for the ZnO-Zn surfaces.

To elucidate these characteristic differences in transistor behavior, we measured the V_G-dependent gate current, I_G, of PIL−EDLTs on both surfaces; these are plotted in Figure 5. The I_G smaller than 200 nA in the IL−EDLTs, as indicated by the blue lines, was noticeably enhanced upon exposure to moisture, indicating that the H^+ and OH^- ions make an important contribution to the I_G. It is clearly shown that the I_G is asymmetric not only for positive and negative biases, but also for the surface termination of the ZnO channels. On the ZnO-Zn surface, the I_G at the negative V_G is larger than the I_G at the positive V_G (Figure 5a), whereas the I_G at the negative V_G is distinctively smaller than the positive side on the ZnO-O surface (Figure 5b). The large I_G and its asymmetric behavior should be closely related to the electrochemical activity of H^+ and OH^- on the ZnO surface. As charged adsorbates, the H^+ and OH^- groups bond to the ZnO surface through chemical or physical adsorption, which depends on the terminating atoms of the ZnO surface. Although a large gate current (charge transfer) flows vertically through the EDL, it has been established that the accumulated Helmholtz layers, whether in the case of IL or PIL, have no direct contribution to the source-drain current, as revealed by the measurements of I_D and V_G at low temperature.[15]

Considering the polarity of ZnO, we propose a surface adsorption mechanism, which is shown in the top panels of Figure 5, for interpreting the origin of the above-mentioned transport behaviors. On the ZnO-Zn surface, the interaction between the H^+ and the terminated Zn atom is rather weak, whereas that between Zn and OH^- is rather strong. When a negative bias is applied to the Pt gate electrode (such that the ZnO channel becomes positive), an oxidation reaction (surface hydroxylation) occurs on the surface, generating a neutral hydroxyl as an adsorbate by giving electrons to the ZnO channel and driving them back to the drain electrode to complete the circuit:

$$\text{ZnO-Zn} + \text{OH}^- \rightarrow \text{e}^- + (\text{ZnO-Zn})-(\text{OH})_{ad} \qquad (1)$$

Since the standard electrode potential, $E(OH^-/OH^0)$, of the surface hydroxylation process is known to be −2.0 V,[36] this surface reaction agrees with the abrupt increase of I_G below −2 V. In contrast, on the ZnO-O surface, the interaction of OH^- with the surface O atom is very weak under negative V_G. When a positive bias is applied to the Pt gate electrode, a reduction reaction (surface hydrogenation) occurs on the ZnO surface, with charges (electrons, e^-) transferred from the ZnO to the proton cation to form neutral hydrogen as an adsorbate:

$$\text{ZnO-O} + \text{e}^- + \text{H}^+ \rightarrow (\text{ZnO-O})-\text{H}_{ad} \qquad (2)$$

The standard electrode potential $E(H^+/H^0)$ is 2.23 V, above which the surface hydrogenation process will occur,[36] which is also in agreement with the observed I_G increasing above +2.2 V.

Briefly speaking, in the case of physisorptions such as $(ZnO-O)\cdots(OH)_{ad}$ and $(ZnO-Zn)\cdots H_{ad}$ bonds, only a small I_G was observed. There should be no charge transfer between adsorbates and surface atoms, which means the adsorption is much closer to an electrostatic process. On the other hand, in the case of $(ZnO-O)-H_{ad}$ and $(ZnO-Zn)-(OH)_{ad}$ bonding, a relatively large I_G was observed because of the strong charge transfer processes between adsorbates and surface atoms (electron transferring processes as described in eqs 1 and 2), indicating the electrochemical sorption processes.

These selective adsorption processes are also responsible for the surface polarity dependent conductivity of the PIL−EDLTs. To reflect the exact conductivities of the adsorbate-modified surfaces, the sheet conductance G_s was deduced from the four-probe measurement. Figure 6 shows the cycle-dependent G_s-V_G curve of the PIL−EDLTs on both surfaces. In the case of the ZnO-Zn surfaces (Figure 6a), the G_s-V_G curve is completely reproducible and cycle independent. These features provide firm evidence that the electron accumulation in the PIL−EDLTs on the Zn-polar surface is mostly electrostatically driven. In marked contrast to the Zn-terminated surface, the ZnO-O surface exhibits a cycle-dependent enhancement of sheet conductivity (Figure

(36) Tomkiewicz, M.; Fay, H. *Appl. Phys.* **1979**, *18*, 1–28.

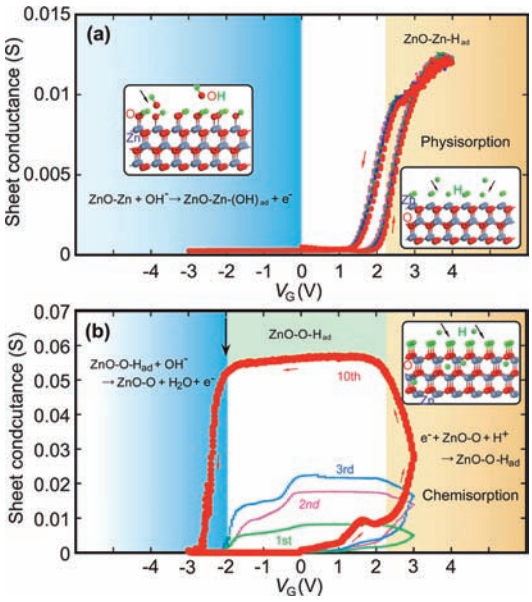

Figure 6. Cycle-dependent sheet conductivities of adsorbed ZnO surfaces. G_s versus V_G curves of PIL−EDLTs on (a) ZnO-Zn surface and (b) ZnO-O surface. Large hysteresis and memory behavior can be obtained on the ZnO-O surface by proton adsorption−desorption processes.

6b). With increased measurement time, the sheet conductivity continues to increase until it reaches the saturation. The maximum conductance at the flat region in a large V_G range reaches 60 mS, which is four times greater than that for the Zn-polar surface. The cycle-dependent transport together with the large hysteresis may indicate that the adsorption mechanism is much more chemical in nature than is the electrostatic case in a ZnO-Zn surface. The high conductance of the ZnO-O surface reminds us of the stability mechanism of hydrogen-terminated polar ZnO surfaces. It has been experimentally and theoretically proved that a ZnO-O surface adsorbed with H via forming a hydrogenated 1×1 pattern to reduce the surface energy shows a metallic conduction behavior.[37−40] The presently observed high conductance is consistent with the research performed in ultrahigh vacuum systems.

More generally, the adsorbed protons and hydroxyls, bonded to a solid surface via charge transfer or electrostatic mechanism, can function as an effective probe for investigating the properties of solid surfaces, particularly on polar solid surfaces. Selectively driving H^+ or OH^- ions to polar surfaces through EDLTs, these charged adsorbates electrostatically or electrochemically interact with surface termination atoms in varied adsorption mechanisms. The resulting distinct variations in electron transport such as gate current and sheet conductance provide us with an easy way to recognize solid surface polarity in a PIL−EDLT configuration.

Proton Memory Performance of PIL/ZnO EDLTs by Proton Adsorption and Desorption. As a charged adsorbate, a proton can bond to a ZnO surface under gate bias through chemisorption or physisorption, relying on the species involved at the EDL interface. As mentioned above, on the ZnO-O surface, the strong O−H bond in (ZnO-O)−H_{ad} adsorption has a large bonding energy around 4.77 eV, involving the chemisorption process between the adsorbate and the surface atoms. Since the (ZnO-O)−H_{ad} bonding is so thermodynamically stable, a large desorption activation energy, namely, a large negative V_G, is required to remove the adsorbed protons from the ZnO surface, causing the large hysteresis in the transfer characteristic (Figure 4b and 6b). This large hysteresis caused by the proton adsorption−desorption processes can be regarded as a memory operation for proton memory devices.

Proton memories have offered an attractive alternative for ultradense, nonvolatile data storage by taking advantage of the lower programmed voltages.[41,42] Compared to existing proton-generating techniques (high-temperature annealing and ion implantation), which can seriously affect logic circuits and cannot control proton concentration,[41,42] our PIL−EDLTs, composed of a proton conductor and a proton trapping surface, show an easier and more reliable way for realizing proton memory transistors. The operation mechanism of the storage element for a proton memory EDLT is depicted in Figure 7, in which the PIL serves as the proton conductor to introduce protons as a medium for the storage element and the ZnO surface functions as a proton trap layer for data storage. Figure 7a shows the original equilibrium state of the device before applying a gate bias; the IL ions are randomly distributed and the hydrogen element still exists in the form of water molecular. No spatial distribution of charges occurs in the PIL. When a positive programming voltage is applied between the gate electrode and the ZnO channel, the protons generated from water dissociation will move to the negatively charged ZnO surface, chemically interact with the surface atoms, and be trapped there (corresponding to surface hydrogenation). As shown in Figure 7b, the resulting spatial redistribution of ionic charges corresponds to the "Write" operation of proton memory. After switching off the positive programming voltage, the trapped protons remain chemically bonded to the ZnO surface because of the large bonding energy, thus, conferring a nonvolatile memory function to the EDLT ("Read" operation, shown in Figure 7c). When a large negative gate voltage is applied, surface hydroxylation occurs and the protons are driven away from the surface. This surface dehydrogenation process on the ZnO surface corresponds to the "Erase" operation, as shown in Figure 7d. On the basis of the above operation mechanism, the memory properties (e.g., erase time, erase voltage, and data

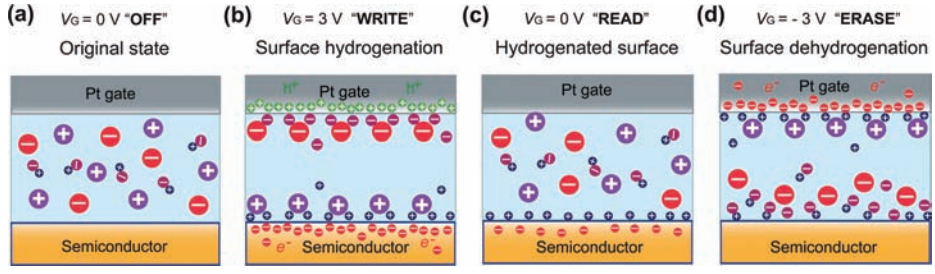

Figure 7. Schematic diagrams of the operation mechanism of a PIL−EDLT memory device. (a) Unbiased state of PIL−EDLT with randomly distributed ions. (b) The "Write" operation (surface hydrogenation). (c) The "Read" operation with a proton-trapped surface. (d) The "Erase" operation (surface dehydrogenation).

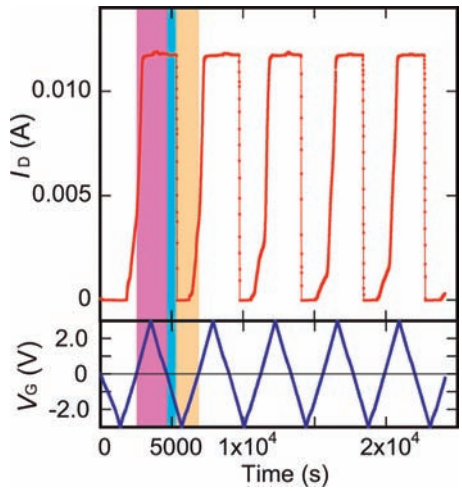

Figure 8. Nonvolatile proton memory behavior of PIL−EDLTs with triangle-shaped gate-voltage scanning. The "Write" operation for data storage is shown in the purple region; the "READ" operation, the blue region; and the "ERASE" operation, the brown region.

retention time) can be modulated by controlling the reversible surface proton-trapping, namely, hydrogenation-dehydrogenation processes.

Figure 8 shows the nonvolatile memory behavior of PIL−EDLTs under triangle-shaped gate bias scanning. One can see that the positive bias applied to the device, where I_D displays an increasing or saturation behavior, functions as the "Write" action for data storage (purple region). At the bias-off state at 0 V where the protons on the ZnO surface still adsorb, I_D maintains the maximum value, which can be regarded as the "READ" operation (blue region). When the gate voltage goes further to a negative value, the proton adsorbates are removed by surface dehydrogenation and I_D suddenly decreases to an OFF state value, which serves as the "ERASE" operation for the storage element (brown region). We note here that the current response to a stepwise gate potential is much quicker than 0.5 s (the measurement interval) in the EDLT even without any device optimization. From the measurement of cycle dependence, the device operation is clearly proved to be reproducible, providing a promising opportunity for practical applications of proton memory devices based on PIL−EDLTs.

Conclusions

In summary, by selectively driving H^+ or OH^- to ZnO channel surfaces through EDL transistors with PIL gating, protons and hydroxyl ions interact with the channel surface atoms in different sorption mechanisms, showing remarkable variations in electron transportation and offering the potential of serving as adsorbate media to extend the functionalities of EDLTs. These functionalies include: (a) increasing EDL capacitance and accumulated carrier density by forming inner Helmholtz layers; (b) realizing surface polarity and surface atom recognition by controlling the chemisorption or physisorption of H^+ and OH^- on polar ZnO surfaces; and (c) achieving proton memory performance via surface hydrogenation. Such findings provide new opportunities for understanding liquid/solid heterogeneous interface phenomena and extending the practical functionality of EDLTs through controllable interfacial interaction.

JA909110S

(37) Woll, C. *Prog. Surf. Sci.* **2007**, *82*, 55–120.
(38) Wander, A.; Harrison, N. M. *J. Chem. Phys.* **2001**, *115*, 2312–2316.
(39) Meyer, B.; Marx, D. *Phys. Rev. B* **2003**, *67*, 035403−1-11.
(40) Kunat, M.; Girol, S. G.; Becker, T.; Burghaus, U.; Wöll, C. *Phys. Rev. B* **2002**, *66*, 081402−1-3.
(41) Vanheusden, K.; Warren, W. L.; Devine, R. A. B.; Fleetwood, D. M.; Schwank, J. R.; Shaneyfelt, M. R.; Winokur, P. S.; Lemnios, Z. J. *Nature* **1997**, *386*, 587–589.
(42) Kapetanakis, E.; Douvas, A. M.; Velessiotis, D.; Makarona, E.; Argitis, P.; Glezos, N.; Normand, P. *Adv. Mater.* **2008**, *20*, 4568–4574.